Building a simple multivariable filtration model to predict irreversible fouling when directly filtering municipal wastewater

Pau Sanchis-Perucho, Jérôme Harmand, Aida Feddaoui-Papin, Daniel Aguado, Ángel Robles

Journal of Environmental Chemical Engineering 12 (2024) 112653

Contents lists available at ScienceDirect

Journal of Environmental Chemical Engineering

journal homepage: www.elsevier.com/locate/jece

Building a simple multivariable filtration model to predict irreversible fouling when directly filtering municipal wastewater

Pau Sanchis-Perucho [a,*], Jérôme Harmand [b], Aida Feddaoui-papin [b], Daniel Aguado [c], Ángel Robles [a]

[a] CALAGUA – Unidad Mixta UV-UPV, Departament d'Enginyeria Química, Universitat de València, Spain
[b] INRAE, UR050, LBE-INRAE, Avenue des étangs, Narbonne, F-11100, France
[c] CALAGUA – Unidad Mixta UV-UPV, Institut Universitari d'Investigació d'Enginyeria de l'Aigua i Medi Ambient – IIAMA, Universitat Politècnica de Valencia, Spain

ARTICLE INFO

Keywords:
Direct membrane filtration
Filtration modelling
Membrane fouling
Municipal wastewater

ABSTRACT

This paper describes a simple generic model designed to predict membrane fouling in municipal wastewater (MWW) treatment. The work was conducted using data from a direct membrane filtration demo-system (middle/long-term filtration periods of about 35 – 124 days) to calibrate the model. Two influents were treated by the demo-system: raw pre-treated MWW and primary settler supernatant from a full-scale MWW treatment plant. A resistance-in-series mathematical model structure was proposed considering fouling due to two different mechanisms: persistent cake layer formation (from suspended material) and pore blocking (from soluble and colloidal compounds). The proposed model represented transmembrane pressure dynamics at different operating solids concentrations (around 1, 2.6, 6 and 11 gL^{-1}) using 7 model parameters, achieving 7–28 mbar differences between the experimental data and model predictions in all cases (calculated as the root mean square error). The model was also able to match the results from two different influents (raw MWW and primary settler supernatant) by modifying 3 of the 7 parameters while low uncertainties were obtained in long-term filtrations, demonstrating its robustness. This model thus provides a good potential to generate reasonable membrane fouling predictions while its simple and open structure makes it easy to implement with complementary materials. Further research will be carried out to enhance the model's precision and validate its potential for optimizing filtration and fouling control processes.

1. Introduction

Membrane technology is achieving ever-increasing interest within the scientific community due to fast and important reductions of acquisition and operating costs together with its significant performance improvements [1]. Its robust and accurate separation capacity, easy scaling-up and low space demands make it an excellent candidate to couple with and enhance the effectivity and feasibility of numerous processes [1]. This is the case of municipal wastewater (MWW) treatment, where systems including membrane technology represents some of the most promising alternatives to achieve sustainable processes [2] (see, for instance, anaerobic membrane bioreactors [3], direct membrane filtration (DMF) [4] or membrane photo-bioreactors [5]). To advance in the successful development and full-scale implementation of the emerging membrane-based technologies, it is necessary to develop complementary tools, such as mathematical models, operational controllers and optimization techniques to allow further understanding of the mechanisms involved in membrane filtration and promote further theoretical studies.

Membrane modelling in MWW treatment is generally based on estimating membrane fouling performance through time in the form of flux declines or transmembrane pressure (TMP) increases. As membrane fouling develops, filtration energy demands also increase, entailing the use of continuous physical and/or chemical fouling control strategies. Minimizing/controlling membrane fouling is usually a key issue to solve in achieving feasible results in these systems [6,7]. Membrane fouling is commonly categorized according to its most relevant source, cake layer formation and pore blocking being the main mechanisms reported [8–10]. Cake layer formation involves the accumulation of particulate material on the membrane surface, which is in proportion to the filtrate volume produced [8,9]. This type of fouling is usually identified as reversible and can be controlled by physical cleaning strategies (*e.g.* gas

* Corresponding author.
E-mail address: pau.sanchis-perucho@uv.es (P. Sanchis-Perucho).

https://doi.org/10.1016/j.jece.2024.112653
Received 8 January 2024; Received in revised form 18 March 2024; Accepted 28 March 2024
Available online 29 March 2024

scouring, crossflow liquid velocity, or backwashing) [11]. Pore blocking (and pore narrowing) describes the partial/complete obstruction of membrane pores by deposits of soluble compounds and/or colloidal particles on the surface or inside the pores, reducing the effective/available membrane filtration area [8,9]. This type of fouling can be either reversible or irreversible (or irrecoverable), depending on the substances involved [11], and its nature can be divided into three sub-categories: (1) standard blocking (narrowed membrane pores due to the internal accumulation of different substances until complete obstruction), (2) intermediate blocking (substances blocking the pores or accumulated on previously deposited materials to form a pseudo cake layer) and (3) complete blocking (substances in the filtered liquor match the membrane pore size and directly block them) [8,9]. Fig. 1 shows a diagram of the different fouling mechanisms. In the specific case of the DMF of MWW, standard/complete pore blocking and cake layer formation have been identified as the main fouling mechanisms [10,12,13], with irreversible fouling dominating the process [12]. Moreover, organic substances have been recognised in numerous studies as the principal fouling source, representing around 70–90% of all the fouling developed in middle/long-term filtrations [12,14–16].

Numerous filtration models have been proposed to model fouling mechanisms based on a resistance-in-series approach [7,17], linking them to specific substances. Unfortunately, despite the significant number of models that can be found in the literature for specific filtration processes, they are in general rather complicated, increasing in complexity as they aim to be general models (*e.g.* [18,19]). Indeed, the large number of physical/chemical interactions that can occur among liquor substances/structure and membrane surface and internal pores still require further research to be properly identified, demanding an understanding and inclusion of multiple unitary steps that result in ever-increasing computational demands. The applicability of these models is therefore complex and limited for purposes of control and optimization (*i.e.* coupling the model to supervising controllers or optimization algorithms) or when combined with biological models in an integrated framework. The development of flexible, simpler and more manageable models is an important milestone in achieving reasonable membrane fouling predictions while allowing easy combination with the complementary materials. Some examples of simple filtration models can be found in [20–22], while filtration optimization and control studies for which they can be used can be found in [23,24]. Unfortunately, they also simplify fouling as the product of a single variable (generally solids concentration in the bulk, see for instance [20,23]), omitting some interesting interactions between pollutants and their impact on fouling development. Building simple multivariable models is thus an interesting field to enhance their prediction capacity and provide more information for potential combinations with complementary tools (supervising controllers or optimization algorithms).

The aim of this work was thus to propose a simple and generic multivariable filtration model to predict membrane fouling under different operating conditions: treated influent, solids concentration and soluble organic compounds (SOC; measured as proteins and carbohydrates) content. A simple and open structure was proposed to allow the easy inclusion of further functions to complement the model according to specific filtration requisites if necessary, while facilitating its integration with other models or process optimization via supervising controllers.

2. Materials and methods

2.1. Filtration experimental data set

The experimental data used to develop the mathematical model was extracted from two former works based on the DMF of MWW using a demo-scale system [12,14]. This data included the experimental results obtained from a filtration plant operated at middle/long-term (from 35 to 124 days per filtration experiment) filtering MWW from different treatment steps of a full-scale facility (*'Conca del Carraixet'* wastewater treatment plant (WWTP), Alboraya-Valencia, Spain). A commercial ultrafiltration membrane module (PULSION® Koch Membrane Systems, 0.03-μm pore size, total filtration area of 43.5 m^2) was used to generate the data set. Membrane fouling was evaluated under two influent sources (*i.e.* raw MWW and the primary settler effluent (PSE) from the cited municipal WWTP) and four operating suspended solids concentrations (around 1, 2.6, 6 and 11 g L^{-1}). The raw MWW was collected from the WWTP's influent after a classic pre-treatment of screening and sieving, desanding and degreasing. The operating transmembrane flux (J) was normalized to 20 ºC in all experiments to mitigate potential viscosity and filterability fluctuations. This approach helped avoid filtration perturbations arising from changes in the temperature of the filtered wastewater. The demo-scale plant operated under consecutive filtration-relaxation stages (F:R), with eventual backwashing (Bw) after 10 completed cycles. Filtration, relaxation and backwashing stages lasted for 300, 60 and 120 s, respectively, giving a F:R:Bw ratio of 50:10:2. Further details on the filtration plant can be found elsewhere [12]. Tables 1 and 2 show the system constants and main influent characteristics used as the model input.

Table 1
System constants.

Constant	Definition	Units	Value
Q (20 ºC)	Permeate flow rate	$m^3\ s^{-1}$	$1.2083{\cdot}10^{-4}$
J (20 ºC)	Transmembrane flux	$L\ h^{-1}\ m^{-2}$	10
A	Total membrane area	m^2	43.5
e_m	Membrane thickness	m	$2.5{\cdot}10^{-3}$
ϵ	Percentage of pores in the membrane	-	0.7
μ (20 ºC)*	Liquid viscosity	$Pa\ s^{-1}$	$1.003{\cdot}10^{-3}$

* A constant liquid viscosity was employed since experimental data were normalized at 20 ℃ in the source work [12,14].

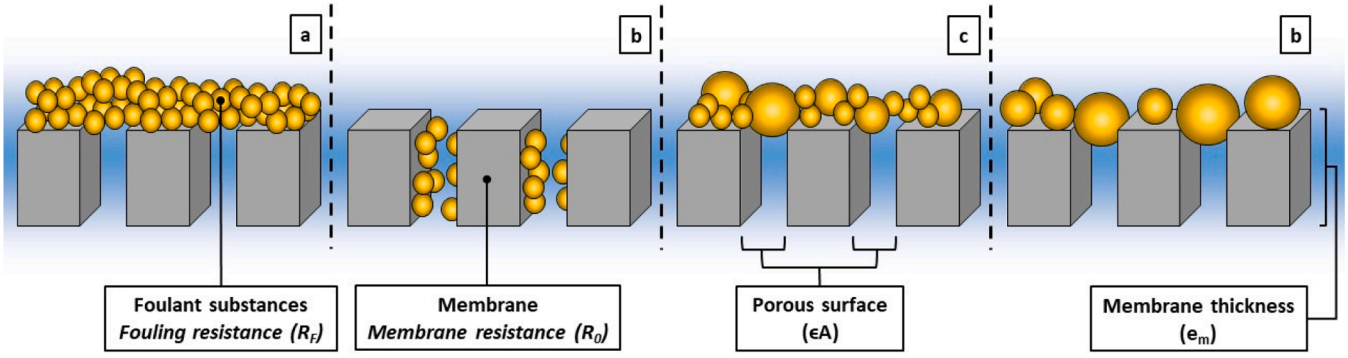

Fig. 1. Fouling mechanism diagram: (a) cake layer, (b) standard pore blocking, (c) intermediate pore blocking and (d) complete pore blocking.

Table 2
Model inputs for each set of experiments.

MWW treated	X_T (g L^{-1})	SOC (mg L^{-1})	R_0*·10^{-12} (m^{-1})
PSE	1.2	78	1.7946
	2.6	101	1.5553
	6.4	116	1.8345
	10.6	97	2.3529
Raw	1.1	96	1.5553
	2.6	109	1.2762
	5.9	127	1.4357
	11.1	142	2.1535

X_T: Suspended solids concentration in the membrane tank. SOC: Soluble organic compounds concentration in the membrane tank measured as proteins and carbohydrates. Raw: Influent municipal wastewater after a classic pre-treatment (screening and sieving, desanding and degreasing). PSE: Effluent of the full-scale wastewater treatment plant primary settler. *R_0 (membrane resistance), calculated from a flux test using the concentrated bulk solution at the beginning of each experimental study.

2.2. Model basics

According to Darcy's law, the relationship between the filtration flux (J) and transmembrane pressure (TMP) in vacuum filtration can be expressed as follows:

$$J = \frac{Q}{A} = \frac{TMP}{\mu \quad R} \tag{1}$$

Where Q is the liquid flow rate, A is the total membrane area, μ is the viscosity of the treated solution, and R is the filtration resistance. In general standings, filtration resistance is given by the addition of two different terms: an intrinsically resistance (R_0) that represents the resistance of the membrane itself to filtration, and the developed fouling resistance (R_F) that represents the increasing filtration resistance with time as membrane fouling develops. R_0 is therefore a constant which can be determined by clean water filtration tests (see for instance [25]) while R_F is a model's variable which needs to be estimated to achieve proper forecasts.

$$R = R_0 + R_F \tag{2}$$

According to the general fouling mechanisms stated above (*i.e.* cake layer formation and pore blocking), this simplified model considers fouling as the result of two independent resistances: (1) the resistance caused by the accumulation of material on the membrane surface (cake layer resistance or R_C), and (2) that linked to the colloidal and soluble compounds attached to membrane pores (pore blocking resistance or R_B). The resulting R_F can then be obtained from the sum of these two resistances:

$$R_F = R_C + R_B \tag{3}$$

Considering the nature of the defined individual resistances, R_C is built as a function of all the suspended material deposited on the membrane surface (defined as m (kg)), while R_B is equivalently built as a function of colloidal and soluble compounds deposited in the membrane pores (defined as n (kg)). The terms m and n are thus the main dynamic variables controlling fouling resistance in the model, which are qualitatively related to the increasing amount of each contaminant accumulated on the membrane during filtration. The following equations are proposed to calculate R_C and R_B:

$$R_C = \alpha' m \tag{4}$$

$$R_B = \alpha'' n \tag{5}$$

Where α' and α'' (m^{-1} kg^{-1}) are model parameters representing the contribution of each fouling compound (m and n) to its specific fouling resistance (R_C and R_B). These model parameters can be directly related to the specific cake layer resistance (α_C, m kg^{-1}) or specific membrane pore blocking resistance (α_B, m kg^{-1}) from classic filtration models (see for instance [26,27]), respectively, when considering the total filtration area (see Eqs. 6 and 7).

$$R_C = \alpha' m = \frac{\alpha_C}{A} m \tag{6}$$

$$R_B = \alpha' n = \frac{\alpha_B}{A} n \tag{7}$$

Eq. 6 and Eq. 7 can be used when at least one of the specific resistances is known, while the simplified expressions (Eq. 4 and Eq. 5) can be used to estimate the qualitative impact of fouling accumulation on filtration resistance when approximations for these physical parameters are not available. In any case, since the total membrane area (A) is a model constant (total filtration area of the membrane module operated), the use of any of proposed expressions will result in the same model outputs.

Based on the work by Benyahia *et al.* [28], the number of pollutants attached to the membrane (*i.e.* m and n) was estimated by considering the mass flux of each related contaminant, proposing the following differential expressions:

$$\dot{m} = \delta_C \quad \frac{Q}{a} \quad X_T \tag{8}$$

$$\dot{n} = \delta_B \frac{Q}{\epsilon a \quad e_m} \quad S \tag{9}$$

Where X_T and S are the concentration of suspended solids and soluble/colloidal material in the bulk, respectively, and 'a' - understand as a(t) - is the dynamic effective filtration membrane area. According to these definitions, δ_C (m^2) is a model parameter involving the impact of the particulate material flux on the cake-layer growth rate, and δ_B (m^3) is its equivalent when considering the soluble and colloidal compounds flux impact on pore blocking growth rate. However, in this latter case, since we only considered the internal surface of membrane pores to be affected by these substances, the effective area is recalculated considering the pores percentage of membrane area (ϵ) and the membrane thickness (e_m). For new membranes, the initial values of m and n will be zero (*i.e.* m(t=0) = 0 and n(t=0) = 0), while these values may be set to the adequate initial conditions for the rest of the cases.

Unlike several studies in the literature on modelling membrane fouling, the proposed model considers that the effective membrane area is not constant during the filtration process, as Benyahia *et al.* [28] proposed. Instead, the membrane permeability loss is reflected not only by an increase in filtration resistance, but also as a reduction of the effective membrane area 'a'. A possible relationship between the fouling accumulation (*i.e.* m and n increases) and the loss of membrane area can be expressed as follows:

$$a = \frac{A}{1 + \frac{m}{\sigma_C} + \frac{n}{\sigma_B}} \tag{10}$$

Where σ_C and σ_B (kg in both cases) are model parameters that consider the effect of each fouling accumulation on membrane area losses. Considering Eq. 2, Eq. 3 and the fouling dynamics link with the dynamic effective membrane area 'a', Eq. 1 can be rewritten as follows:

$$J = \frac{Q}{a} = \frac{TMP}{\mu \quad (R_0 + R_C + R_B)} \tag{11}$$

According to the proposed model, greater fouling accumulation during filtration means that a smaller membrane area is available for continuing with the process, increasing consequently the operating filtration flux, since a smaller effective membrane area is used to treat the same liquid flow rate. This dynamic then creates a circular interaction between m and n and the effective membrane area 'a', which is

the basic loop used by the model to estimate fouling development.

2.3. Further model considerations

As stated above, the model estimates fouling from the dynamics between *m*, *n* and *'a'*. However, it does not include any mechanisms to reduce fouling in the system, which means that all the developed fouling was considered as irreversible. This was appropriate for the results modelled in this work, since the experimentally observed fouling was determined to be mostly irreversible [12,14]. Indeed, backwashing and air sparging showed an irrelevant effect on fouling control in the cited works. Then, the experimental backwashing phases were modelled in this work as relaxation stages. In addition, since cake layer fouling is generally considered mainly reversible, the term 'persistent cake layer' will be used from this point forward in the manuscript to refer to the R_C resistance. It could be defined as the remnants of the formed cake layer not able to detach by mechanical forces (*i.e.* irreversible fouling developed from particles attached to the membrane surface).

On the other hand, since only data concerning SOC concentration during filtration were available, the membrane pore blocking resistance was completely linked to the total concentration of these substances in this work, expressing Eq. 9 as follows:

$$\dot{n} = \delta_B \frac{Q}{\epsilon a \quad e_m} \quad SOC \tag{12}$$

However, given all the different soluble and colloidal substances that can interact with membrane filtration according to the bulk characteristics, the following generalized expression can be proposed to consider their overall effect on the model (Eq. 9):

$$\dot{n} = \delta_B \frac{Q}{\epsilon a \quad e_m} \quad \sum_{i=1}^{N} (f_i \quad x_i) \tag{13}$$

Where N is the number of soluble and colloidal materials considered in the process, *x* represents their concentration, and *f* represents the relative relevance of each considered soluble and colloidal compound over total relevance (*i.e.* $\sum_{i=1}^{N} f_i = 1$).

Finally, the data set used revealed that an increase in the bulk suspended solids concentration had a sharp beneficial effect on the overall filtration performance, achieving less fouling growth rates (see [12,14]). This phenomenon was attributed to the formation of thicker cake layers during filtration, which prevented the soluble substances and colloids reach the membrane surface, as other authors have also theorized [29–31]. Since increasing the solids concentration (X_T) reduced the fouling propensity related to these substances ($\dot{n}$), an inhibition function for pore blocking was included in the model (Eq. 12) to consider this effect. In this case, a classic literature exponential inhibition function [32] was used due to the good fits obtained for the studied experimental data set. However, other inhibition functions, or none, could be proposed, depending on the process, if necessary. Eq. 12 can then be rewritten as follows:

$$\dot{n} = \delta_B \frac{Q}{\epsilon a \quad e_m} \quad SMP \quad e^{-k_I} \quad x_T \tag{14}$$

Where k_I (kg^{-1}) is an inhibitor constant which needs to be determined as a model parameter from experiments.

2.4. Model implementation, calibration and validation

The model was implemented in MATLAB®. Function 'ODE45' was used for the differential equations operations. The experimental average TMP calculated for each operating day was used to calibrate the model from the data set. The experimental data from the operating solids concentration of about 1, 2.6 and 6 g L^{-1} were used for calibration, leaving all the experimental data from a solids concentration of about 11 g L^{-1} for validation. The low concentration experimental data (*i.e.* 1 and 2.6 g L^{-1}) were used for calibration due to the high TMPs obtained in those experiments, providing sufficient information for proper parameter calibration. Consequently, only data from 6 and 11 g L^{-1} could be used for validation. Using the 11 g L^{-1} data for validation was preferred to add more credibility to the model, as these results lie outside the operating limits used during calibration, thereby enhancing its validity. However, it is worth mentioning that similar parameter values were obtained when using the 11 g L^{-1} data for calibration (data not shown), rendering the choice of which set of experiments to use for calibration (*i.e.* 6 or 11 g L^{-1}) inconsequential.

Two different sets of parameters were calibrated for each MWW evaluated (*i.e.* raw and PSE). The error between the experimental TMP (TMP_{exp}) and the predictions obtained from Eq. 11 (TMP_{teo}) was used as the objective value for parameter calibration, minimizing its value by using a nonlinear optimization algorithm function ('fmincon', MATLAB/Simulink). The error was calculated as the root mean square error (RMSE):

$$RMSE = \sqrt{\frac{\sum_{i=1}^{N} \left(TMP_{\exp} - TMP_{teo}\right)^2}{N}} \tag{15}$$

Where N represent the total amount of data.

On the other hand, the theoretical study of the identifiability of the model can be difficult and laborious. To ensure its practical identifiability, a procedure in which parameter optimization was obtained from several sets of initial conditions was adopted. By limiting the number of parameters to be identified (chosen by a sensitivity study), it was guaranteed to obtain a single set of parameters for each experimental condition tested [33].

2.5. Sensitivity and uncertainty analysis

Two global sensitivity analyses (GSA) were applied to determine the model's most influential parameters after calibration: the standardized regression coefficient method (SRC) and Morris screening method [34]. In both methods, an input variation factor of ±10% regarding default values (see Table 3) was considered. SRC was performed according to the Monte Carlo method, applying semi-random Latin Hypercube Sampling [35] to generate parameter variations. The number of Monte Carlo simulations was set to 2000. Inputs resulting in standard regression coefficients (β_i) higher than 0.1 were considered as influential factors, establishing a minimum coefficient of determination (R^2) of 0.7 to validate β_i as a sensitivity measure [36]. The Morris method was conducted by the scaled elementary effect (SEE_i) proposed by Sin and Gernaey [37]. The trajectory-based sampling strategy proposed by Ruano *et al.* [38] was used as a modification of the Morris screening method to improve the calculation of SSE_j finite distribution associated with each input factor (F_j). The absolute mean (μ*, Eq. 16) and standard deviation (σ, Eq. 17) were used as statistical parameters to determine the relative importance of parameter variations on the model's output [36,

Table 3
Calibrated parameters.

Parameter	Units	MWW		DBP (%)
		PSE	Raw	
α'	$m^{-1}\ kg^{-1}$	$2{\cdot}10^{12}$	$2{\cdot}10^{12}$	-
α''	$m^{-1}\ kg^{-1}$	$2{\cdot}10^{12}$	$2{\cdot}10^{12}$	-
δ_C	m^2	$1.6198{\cdot}10^{-3}$	$8.4963{\cdot}10^{-4}$	47.55
δ_B	m^3	$7.8223{\cdot}10^{-3}$	$3.1933{\cdot}10^{-3}$	59.18
σ_C	kg	1	1	-
σ_B	kg	1	1	-
k_I	kg^{-1}	0.6436	0.3945	38.70

DBP: Difference between the parameters calibrated for the two MWWs studied. Raw: Influent municipal wastewater after a classic pre-treatment of screening and sieving, desanding and degreasing). PSE: Effluent of the full-scale wastewater treatment plant primary settler

39].

$$\mu_i^* = \frac{\sum_{j=1}^{r} |SEE_j|}{r} \quad (16)$$

$$\sigma_i = \sqrt{\frac{1}{r}\sum_{j=1}^{r} (SEE_j - \mu_i)^2} \quad (17)$$

Where r is the number of trajectories evaluated (set to 100 in this study) and μ is the mean. A resolution of p=4 was used [40]. Morris total simulations (MTS) were calculated by Eq. 18, ascending in this case to 800.

$$MTS = r(k+1) \quad (18)$$

Where k is the number of input factors (*i.e.* analysed parameters; 7 in this study: α', α'', δ_C, δ_B, σ_C, σ_B and k_I).

The uncertainty analysis (UA) of the model was studied after the identification of its most sensible parameters. A parameter variation factor of ±10% regarding default values (see Table 3) was applied. This analysis was conducted by determining the 5th and 95th percentiles of the Monte Carlo simulations [41].

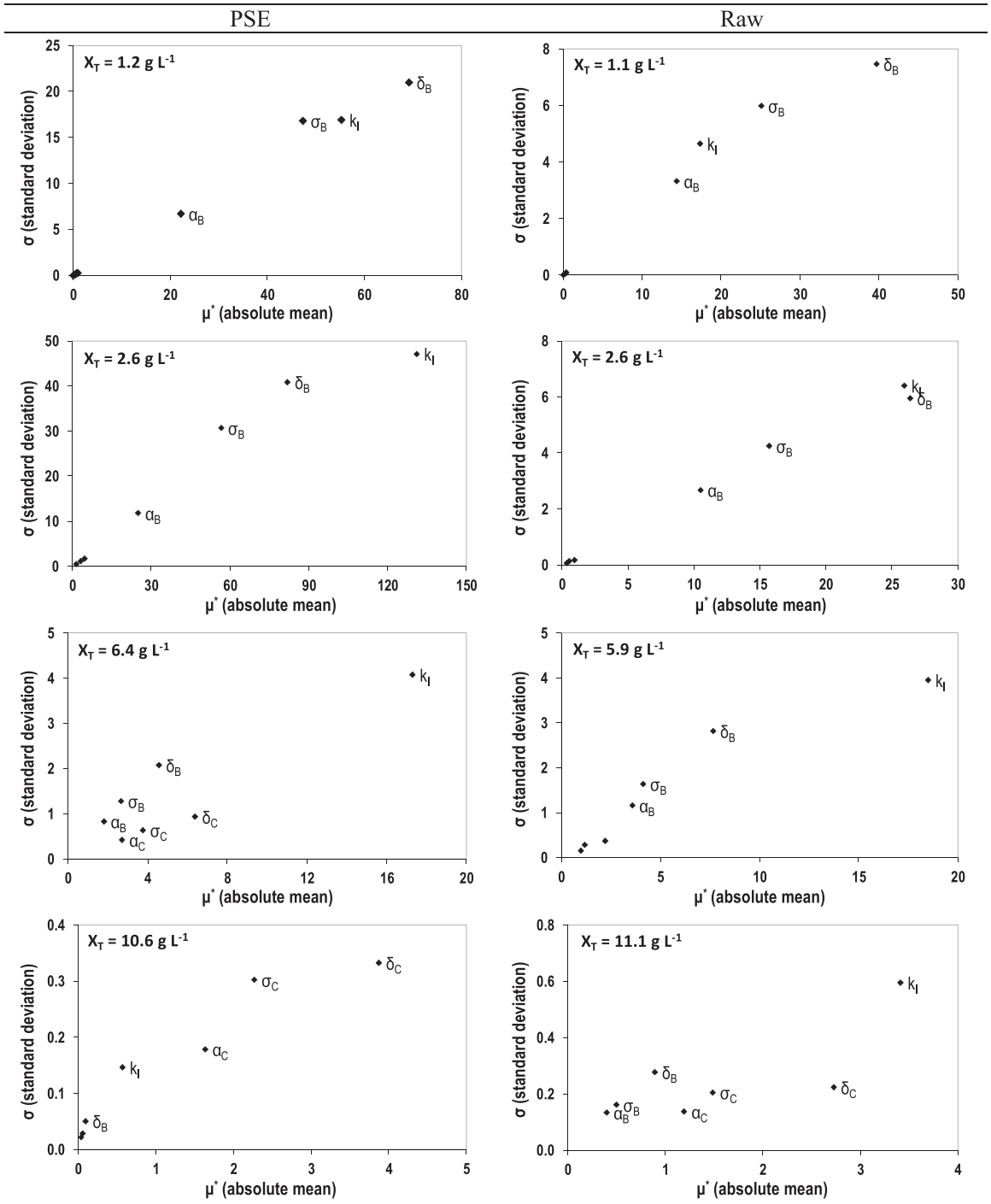

Fig. 2. Results of the Morris screening method. Same simulation time of that reached by each filtration experimental set was used to evaluate the parameter's sensitivity. Raw: Influent municipal wastewater after classic pre-treatment (screening and sieving, desanding and degreasing). PSE: Effluent from the full-scale wastewater treatment plant primary settler.

3. Results and discussion

3.1. Sensitivity and identifiability analysis

Table 3 shows the model parameters values after calibration. Overall, the SRC sensitivity study identified 3–4 of the 7 model parameters as influential model factors depending of the case (see Fig. S1). This method suggests that δ_B, σ_B, α'' and k_I (all related to the mass of SOC attached the membrane) are important input factors when operating at low solid concentrations (around 1 and 2.6 g L^{-1}), while their influence declines when operating at higher solids concentrations (above 6 g L^{-1}), regardless of the MWW treated. In this second case, parameters related to the particulate material fouling (*i.e.* δ_C, σ_C, α') control the model output (See Fig. S1). As will be discussed in Section 3.2, the TMP was mainly controlled by soluble compounds fouling (n) in the low solids concentration range, becoming less important as bulk solids

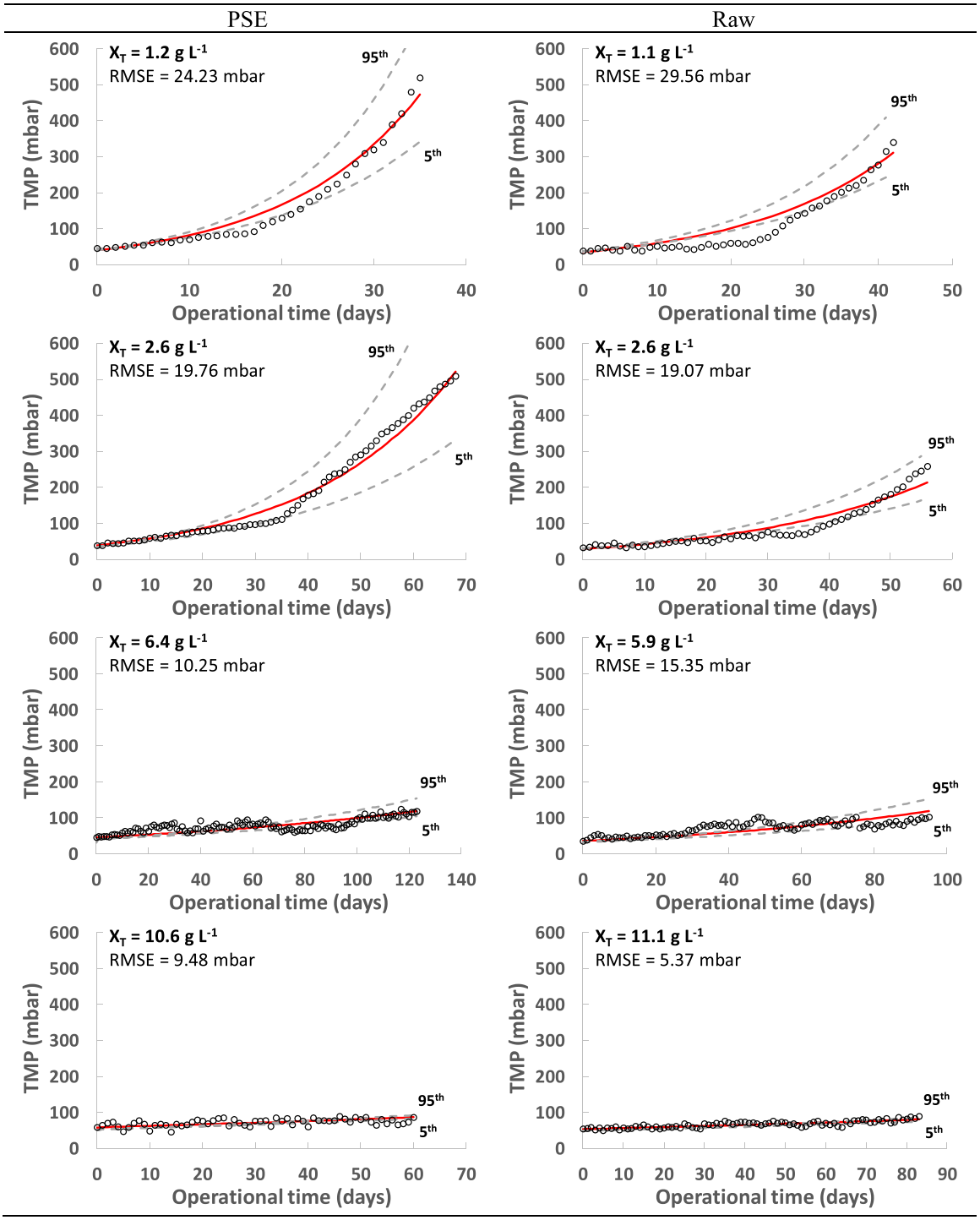

Fig. 3. Model's TMP predictions in the middle/long-term: (a) TMP evolution and (b) model variables' evolution. Experimental data are shown by dots while the model's predictions are shown by lines. The 5th and 95th represent the corresponding uncertainty percentiles from the Monte Carlo simulations. Note that each figure includes the experimental operating solids concentration. Two MWW were studied: PSE (effluent from the full-scale wastewater treatment plant primary settler) and Raw (influent municipal wastewater after classic pre-treatment of screening and sieving, desanding and degreasing).

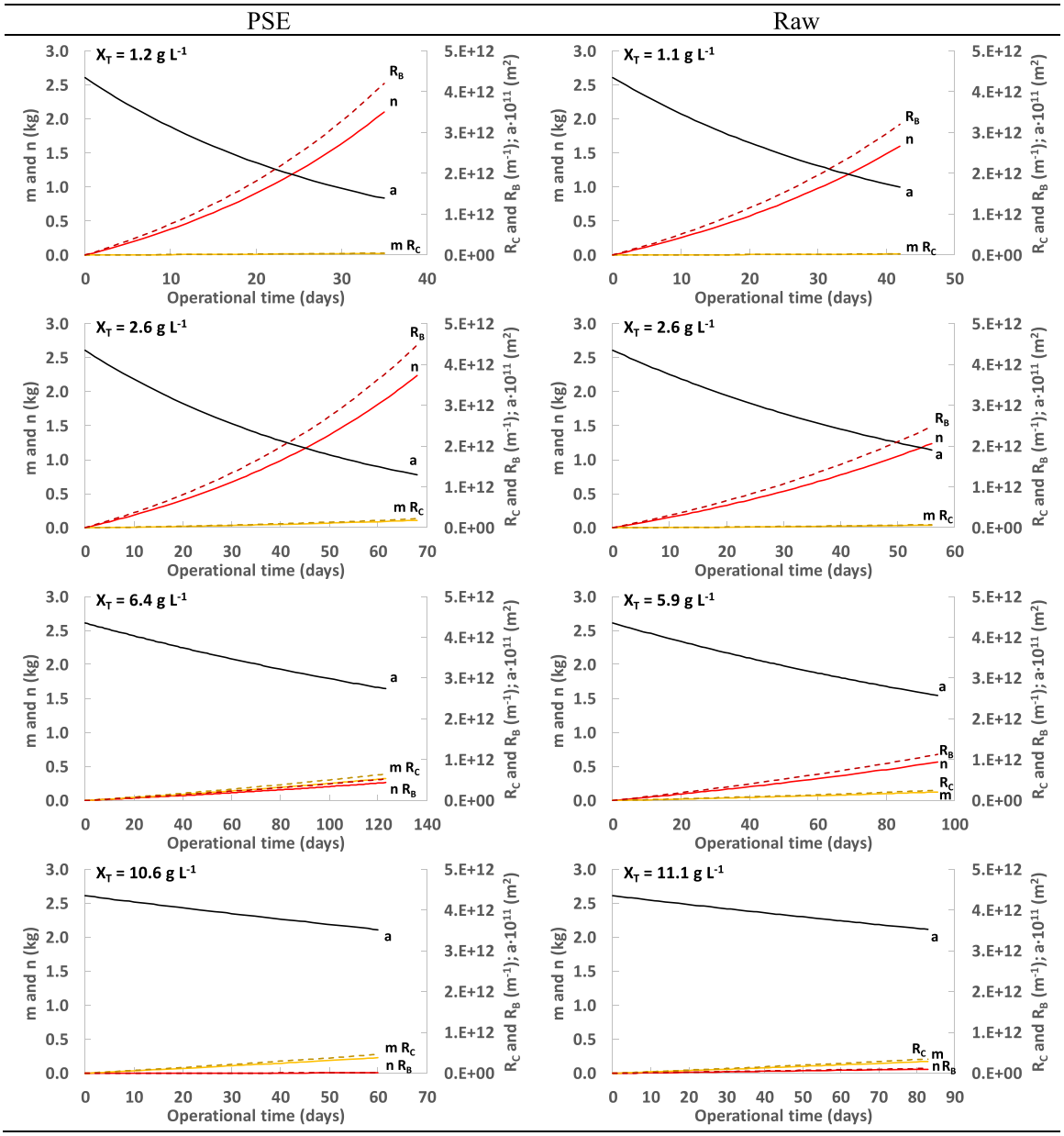

Fig. 3. (*continued*).

concentration rose. Consequently, the higher the operating solids concentration in the membrane tank, the less the degree of *n*-related fouling. Unfortunately, low degrees of correlation were obtained between the variations in parameter values and the subsequent effects on the model output (see Fig. S1), which steadily declined as the simulation time was increased. Since the SRC method demands correlations above 0.7 to validate the sensitivity results [36], it was not possible to validate this method in any of the evaluated scenarios, mainly due to the nonlinearity of the model presented. Nevertheless, since similar results were obtained by the Morris screening method, results from short simulations could be used in this case to identify the sensible parameters.

Likely the SRC, the Morris screening method also revealed that 4 out of 7 model parameters (mainly δ_B, σ_B, α'' and k_I) were influential on the model output (see Fig. 2), although as in the SRC evaluation, parameters related to particulate material fouling (*i.e.* δ_C, σ_C, α') also gained importance as raising the solids concentration in the bulk (see Fig. 2).

The identifiability analysis indicated that the proposed set of parameters was 4 degrees of freedom higher than the level required in this case, due to the lack of information on fouling development in the studied experimental sets. In fact, no information was available on the specific cake layer resistance during the process or the level of pollutants attached to the membrane. Consequently, only a qualitative evolution of the pollutants accumulated on the membrane surface or in the pores (*i.e.* *m* and *n* evolution) could be expected from the model in this case. To solve this identifiability issue, the value of 4 of the less-sensitive parameters (σ_C, σ_B, α' and α'') was set to a constant value to reduce the degrees of freedom: 1 kg for parameters σ_C and σ_B and $2{\cdot}10^{12}$ m^{-1} kg^{-1} for parameters α' and α''. The number of parameters to be calibrated was consequently reduced to 3 (δ_C, δ_B and k_I).

3.2. Model performance and uncertainty analysis

Fig. 3a shows the model performance for the tested operating conditions (calibrated parameters values can be found in Table 3), while R_C, R_B, *m*, *n* and '*a*' evolutions are shown in Fig. 3b to allow an easier interpretation of the model performance. Reasonably good fits were

obtained in all cases, achieving low RMSE values between about 7 – 28 mbar. Good fits were also obtained during model validation (solid concentration of about 11 g L^{-1}), showing the model's good prediction capacity (see Fig. 3a). As stated above, this model is based on the interaction between fouling accumulation and the membrane's loss of permeability (*i.e.* *m* and *n* increase and '*a*' declines), creating dynamics in which the effective operating flux virtually increases due to the reduced effective membrane filtration area. This membrane permeability reduction can be in two different ways: a persistent cake layer formation (related to *m*) and pore blocking (related to *n*), since '*a*' is affected by both in the same way (see Eq. 10). The described dynamic can be appreciated in Fig. 3b, where a decline in '*a*' can be observed as filtration advances, regardless of the major fouling source changing due to the modified operating solids concentration. Fouling was primarily controlled by pore blocking at low operating solids concentrations (around 1 and 2.5 g L^{-1}), while persistent cake layer formation dominated fouling otherwise (*i.e.* at operating solids concentrations about 6 and 11 g L^{-1}). This shift can be clearly appreciated in the greater increases of *n* and R_B at the low solids range (around 1 and 2.5 g L^{-1}), transitioning to dominance by *m* and R_C as the operating solids concentration increased (see Fig. 3b). This dynamic was achieved by incorporating a pore-blocking inhibition function into Eq. 14, as detailed in Section 2.3, in alignment with the findings of Sanchis-Perucho *et al.* [12,14].

On the other hand, similar values for the considered model parameters were reached after calibrating the model for the influents studied (raw and PSE), as shown in Table 3. This was presumably due to the two studied MWWs sharing the same matrix, *i.e.* PSE obtained from raw MWW after the primary settling step. The lower fouling rate propensity when treating raw MWW instead of PSE (see Fig. 3) was captured by the model through a lower value for the δ_C and δ_B parameters. However, these differences could have arisen from oversimplifying the pollutants that promote fouling. As suggested by Sanchis-Perucho *et al.* [12,14], the particle size distribution of the filtered bulk is a key factor in membrane fouling propensity when directly filtering untreated non-biological MWW. Including information on the colloidal fraction concentration (which has been identified as an important fouling promoter [42]) and the average particle size of the bulk suspended solids particles could thus significantly enhance this model's fouling prediction capacity. Further studies will be required on this latter point to develop a more complete model capable of predicting fouling from the two influents studied using a single set of parameters.

Finally, the UA performed when considering the most influential model parameters in each case showed that low uncertainties can be expected when the operating TMP is held below 150–200 mbar, steadily increasing as the fouling occurring in the membrane raises (see Fig. 3a). This is because future fouling development in filtration systems strongly depend on past fouling conditions. Consequently, minimal divergence during parameters calibration could lead to substantial discrepancies in the long-term due to cumulative errors. Nonetheless, the uncertainties obtained by the model showed no more than 100 – 150 mbar differences in the latter stages of filtration (*i.e.* when the available membrane area '*a*' approached to 0). Slight errors in the parameters calibration will thus not heavily impact on the model's prediction capacity, showing its robustness.

3.3. Forecasts when increasing the solids concentration in the bulk and potential applications of the model

As aforementioned, the proposed model was built to consider the beneficial effects of increasing the solids concentration in the bulk on mitigating pore-blocking fouling. However, many membrane systems operate at much higher solids concentrations than those reached in the experimental data set used, wherein an increase in solids concentration entails higher fouling propensities [11,43]. To estimate the model outputs when operating at higher solids concentrations than those evaluated in this work and to assess its suitability for matching other filtration results, a number of simulations were performed. These simulations involved determining the final TMP achieved after 150 days of filtration, with the solids concentration increased in each case from 1 to 20 mg L^{-1} (solids increment step of 1 mg L^{-1}), totalling 20 independent simulations. Parameters calibrated from PSE filtration were used in these simulations, considering a constant SOC concentration in the bulk of 16 mg L^{-1}.

Fig. 4 shows the results obtained when simulating this steady increase in the operating solids concentration in the filtered bulk. A changing dynamic was observed for the forecasted TMP, initially decreasing but later increasing as the solids concentration rose to over 4–5 g L^{-1} (see Fig. 4a). This change was due to the shift in the primary fouling contributor from pore blocking '*n*' to persistent cake layer '*m*', as anticipated with the increase in solids (see Fig. 4b). These results demonstrate the existence of an optimal solids range: initially enhancing filtration by preventing pore-blocking fouling but hindering it due to the increasing persistent cake layer fouling with further increments in concentration. This model could thus be particularly interesting for determining the optimum solids range when directly filtering MWW, which may be strongly influenced by other operating conditions such as the SOC concentration in the bulk or the transmembrane flux. On the other hand, its outcome when raising solids concentration suggests that the model could potentially match results from other filtration systems where solids concentration dominates fouling. The model could

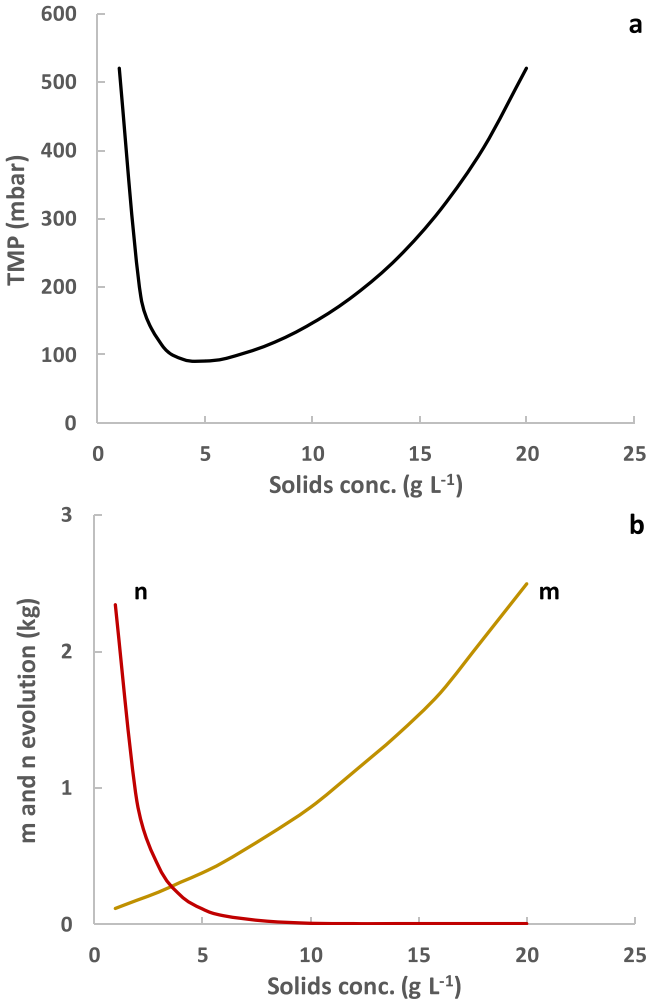

Fig. 4. Simulation runs when increasing solids concentration using parameters calibrated for PSE treatment (see Table 3). All simulations were performed at 150 days of filtration at a constant SOC concentration of 16 mg L^{-1}.

therefore be tested for other applications, such as MBRs, and even coupled with complementary biological models to predict irreversible membrane fouling in those systems. Examples and guidelines for similar simple models applied to MBRs can be found in [22,28]. In the case of applying this model to other membrane systems, were reversible fouling could be more relevant, the effects of the applied fouling control strategies would be adsorbed by a lower propensity to irreversible fouling in the system (*i.e.* a lower value for parameters δ_C and δ_B). Consequently, although this model does not give proper short-term predictions (*i.e.* when just few cycles of filtration-relaxation are simulated), it could produce proper results when considering the average TMP in the middle/long-term. Regarding the integration of this model with supervisory controllers, it could be utilized to determine the optimal set points of the filtration process via optimization algorithms. This process entails selecting the most significant process variables for dynamic control and optimization with the aim of minimizing fouling development and operating costs. The optimization is based on predictions derived from the model, with inputs such as influent MWW characteristics being regularly updated. Examples and guidelines of this kind of applications in MBRs can be found in [44,45]. Further studies are needed to evaluate all these potential applications of the model mentioned above.

3.4. Merits, limitations and challenges of the model

The presented model was able to produce reasonable fouling predictions for the data evaluated in this work. Furthermore, Fig. 4 demonstrates the model's potential to match the different types of fouling behaviour described in the related literature thanks to the proposed dynamics between *m*, *n* and '*a*', maintaining nevertheless a simple and open structure. Other simple models can be found in literature to predict membrane fouling in MBRs [20,22,23,28], achieving also good performances when combined with biological processes. However, these generally consider fouling as the product of a single variable (usually solids concentration in the bulk, see for instance [20,23]), shortening their applicability range. This model contributes therefore to overcoming this shortcoming, providing membrane fouling predictions based on two variables and their potential interaction with each other. In addition, to the best of the authors' knowledge, no filtration models specialized on the DMF o MWW can be found in the literature, this being a first tentative in the field. In fact, filtration models are usually built either for general, not specific applications, or with MBRs in mind, their adaptation to the DMF of MWW obliging to adapt and/or include more functions and/or to increase their number of parameters and complexity. General filtration models could also be evaluated to match these experimental results, since they are also mainly based on physical interactions between pollutants and the membrane (see for instance [9, 46]). However, their adaptation would also require an increase in the model's complexity, including considerations such as cake layer porosity and compressibility [46–48] or collisions and agglomerations between particles [49,50]. Moreover, the particle size distribution of the influent feed, which is usually required in these models [47–50], is not a simple parameter to continuously monitor. Indeed, it can be highly variable, and specialized equipment is required for its determination. Instead, this model presents an extremely simple structure, requiring only the calibration of 3 parameters in this work to achieve proper results, while solids and SOC (proteins and carbohydrates) are extensively used variables that can easily be determined via classic methods or commercial kits. This makes the proposed model an interesting tool for filtration control in this field due to its simplicity and easy implementation or its ability to combine with other tools (*e.g.* complementary supervising controllers or optimization algorithms).

Despite the aforementioned merits, the simplicity of the proposed model also entails significant limitations that need to be considered. Since the model only predicts irreversible fouling, short-term optimization of filtration operating conditions is not possible. Indeed, reversible cake layer dynamics are omitted in this model, making it unsuitable for systems where controlling reversible fouling is a major priority. Likewise, the model lacks the capacity to predict fouling dynamics resulting from changes in the particle size distribution of the feed and/or the pore size of the membrane used. Therefore, this model is not recommended for processes where the quality of the influent experiences significant fluctuations in particle size or nature. Finally, the effect of changing fouling control strategies is not considered. While this may not be a significant issue as such strategies typically focus on mitigating reversible fouling, if they change significantly affect the occurrence of irreversible fouling in the applied system, a recalibration of the model parameters according to the new operating conditions would be necessary.

Further research is planned to address some of the aforementioned limitations. For example, the incorporation of reversible cake layer dynamics could be considered by distinguishing between reversible and irreversible cake layer formations in the model, similar to other existing models [51]. Additional functions could also be introduced to mitigate reversible cake layer formation, taking into account the impact of various reversible fouling control strategies, such as in multiple filtration models [20,28,51]. Moreover, the average particle size distribution of the feed could be included as a model variable, as in [47–50], aiming to account for the effects of the influent MWW filtered under a unified set of parameters, as proposed in Section 3.1. However, these potential enhancements would likely increase the complexity of the model, potentially compromising its primary strength and focus, simplicity. Therefore, comprehensive research is necessary to determine whether integrating some of these proposed modifications is justified. Additionally, further studies are required to improve the accuracy of the model's predictions for various filtration conditions (*e.g.* direct MWW filtration at higher solids concentrations and different permeate fluxes), while it is essential to evaluate the model's performance in other filtration systems or when utilized as an optimization/control tool for filtration.

4. Conclusions

This paper proposes a simple generic model with 7 calibration parameters to predict long-term membrane fouling in direct MWW filtration. Good predictions were obtained for different operating solids concentrations (about 1, 2.6 and 6 g L^{-1}), achieving RMSE values between the experimental data and model predictions of around 7 – 28 mbar. Good fits were also obtained when applying the calibrated model to a higher solids concentration (about 11 g L^{-1}), validating the proposed model for a short solids concentration range. The model was also able to match the results from two different influents (raw municipal wastewater and the effluent of the primary settler) by simply modifying 3 of the 7 parameters while the uncertainly analysis showed that slight uncertainties can be expected in long-term simulations, demonstrating the robustness of the model. The proposed model demonstrates thus a good potential in generating reasonable membrane fouling predictions. Its key strengths lie in its ability to account for fouling from two distinct sources (solids and SOC), also considering their combined effect on membrane permeability decline, while maintaining an extremely simplistic and adaptable structure, facilitating its integration with other complementary materials. Moreover, to the best of the authors' knowledge, no filtration models specialized on the DMF o MWW can be found in the literature, this being a first tentative in the field. Further studies will be conducted to enhance the accuracy and broaden the application range of the model, as well as to validate its potential for optimizing filtration systems and controlling fouling.

CRediT authorship contribution statement

Pau Sanchis-Perucho: Writing – original draft, Software, Methodology, Investigation, Formal analysis, Data curation. **Aida Feddaoui-papin:** Writing – review & editing, Supervision. **Jérôme Harmand:**

Writing – review & editing, Validation, Supervision, Resources, Methodology. **Daniel Aguado:** Writing – review & editing, Supervision, Funding acquisition. **Angel Robles:** Writing – review & editing, Supervision, Software, Resources, Methodology.

Declaration of Competing Interest

The authors declare that they have no known competing financial interests or personal relationships that could have appeared to influence the work reported in this paper.

Data Availability

Data will be made available on request.

Acknowledgements

This research work was supported by the Ministerio de Economia, Industria y Competitividad via Grant Nº PRE2018-083726. It was also made possible thanks to the financial support received from the above Ministry during the implementation of the Project "*Aplicación de la tecnología de membranas para potenciar la transformación de las EDAR actuales en estaciones de recuperación de recursos*." (CTM2017–86751-C1 and CTM2017–86751-C2).

Appendix A. Supporting information

Supplementary data associated with this article can be found in the online version at doi:10.1016/j.jece.2024.112653.

References

[1] S.P. Bera, M. Godhaniya, C. Kothari, Emerging and advanced membrane technology for wastewater treatment: a review, J. Basic Microbiol. 62 (2022) 245–259, https://doi.org/10.1002/jobm.202100259.
[2] M. Issaoui, S. Jellali, A.A. Zorpas, P. Dutournie, Membrane technology for sustainable water resources management: challenges and future projections, Sustain. Chem. Pharm. 25 (2022) 100590, https://doi.org/10.1016/j.scp.2021.100590.
[3] S. Vinardell, S. Astals, M. Peces, M.A. Cardete, I. Fernández, J. Mata-Alvarez, J. Dosta, Advances in anaerobic membrane bioreactor technology for municipal wastewater treatment: a 2020 updated review, Renew. Sustain. Energy Rev. 130 (2020), https://doi.org/10.1016/j.rser.2020.109936.
[4] A. Jiménez-Benítez, P. Sanchís-Perucho, J. Godifredo, J. Serralta, R. Barat, A. Robles, A. Seco, Ultrafiltration after primary settler to enhance organic carbon valorization: energy, economic and environmental assessment, J. Water Process Eng. 58 (2024), https://doi.org/10.1016/j.jwpe.2024.104892.
[5] H. Zou, N.C. Rutta, S. Chen, M. Zhang, H. Lin, B. Liao, Membrane photobioreactor applied for municipal wastewater treatment at a high solids retention time: effects of microalgae decay on treatment performance and biomass properties, Membr. (Basel) 12 (2022), https://doi.org/10.3390/membranes12060564.
[6] M.K. Shahid, A. Kashif, P.R. Rout, M. Aslam, A. Fuwad, Y. Choi, R. Banu J, J. H. Park, G. Kumar, A brief review of anaerobic membrane bioreactors emphasizing recent advancements, fouling issues and future perspectives, J. Environ. Manag. 270 (2020) 110909, https://doi.org/10.1016/j.jenvman.2020.110909.
[7] Á. Robles, M.V. Ruano, A. Charfi, G. Lesage, M. Heran, J. Harmand, A. Seco, J. P. Steyer, D.J. Batstone, J. Kim, J. Ferrer, A review on anaerobic membrane bioreactors (AnMBRs) focused on modelling and control aspects, Bioresour. Technol. 270 (2018) 612–626, https://doi.org/10.1016/j.biortech.2018.09.049.
[8] A. Alborzi, I.M. Hsieh, D. Reible, M. Malmali, Analysis of fouling mechanism in ultrafiltration of produced water, J. Water Process Eng. 49 (2022) 102978, https://doi.org/10.1016/j.jwpe.2022.102978.
[9] B. Huang, H. Gu, K. Xiao, F. Qu, H. Yu, C. Wei, Fouling mechanisms analysis via combined fouling models for surface water ultrafiltration process, Membr. (Basel) 10 (2020) 1–12, https://doi.org/10.3390/membranes10070149.
[10] T. Fujioka, L.D. Nghiem, Fouling control of a ceramic microfiltration membrane for direct sewer mining by backwashing with ozonated water, Sep. Purif. Technol. 142 (2015) 268–273, https://doi.org/10.1016/j.seppur.2014.12.049.
[11] X. Du, Y. Shi, V. Jegatheesan, I.Ul Haq, A review on the mechanism, impacts and control methods of membrane fouling in MBR system, 2020. https://doi.org/10.3390/membranes10020024.
[12] P. Sanchis-Perucho, D. Aguado, J. Ferrer, A. Seco, A. Robles, Direct membrane filtration of municipal wastewater: studying the most suitable conditions for minimizing fouling growth rate in porous membranes, SSRN Electron. J. (2022), https://doi.org/10.2139/ssrn.4191277.
[13] S. Hube, J. Wang, L.N. Sim, T.H. Chong, B. Wu, Direct membrane filtration of municipal wastewater: linking periodical physical cleaning with fouling mechanisms, Sep. Purif. Technol. 259 (2021), https://doi.org/10.1016/j.seppur.2020.118125.
[14] P. Sanchis-perucho, D. Aguado, J. Ferrer, A. Seco, Á. Robles, Evaluating resource recovery potential and process feasibility of direct membrane ultrafiltration of municipal wastewater at demonstration scale, Environ. Technol. Innov. 32 (2023) 103252, https://doi.org/10.1016/j.eti.2023.103252.
[15] K. Kimura, D. Honoki, T. Sato, Effective physical cleaning and adequate membrane flux for direct membrane filtration (DMF) of municipal wastewater: up-concentration of organic matter for efficient energy recovery, Sep. Purif. Technol. 181 (2017) 37–43, https://doi.org/10.1016/j.seppur.2017.03.005.
[16] T.A. Nascimento, F.R. Mejía, F. Fdz-Polanco, M. Peña Miranda, Improvement of municipal wastewater pretreatment by direct membrane filtration, Environ. Technol. (U. Kingd.) 38 (2017) 2562–2572, https://doi.org/10.1080/09593330.2016.1271017.
[17] G.Di Bella, D.Di Trapani, A brief review on the resistance-in-series model in membrane bioreactors (MBRs), Membr. (Basel) 9 (2019), https://doi.org/10.3390/membranes9020024.
[18] J. Busch, A. Cruse, W. Marquardt, Modeling submerged hollow-fiber membrane filtration for wastewater treatment, J. Memb. Sci. 288 (2007) 94–111, https://doi.org/10.1016/j.memsci.2006.11.008.
[19] X. yan Li, X. mao Wang, Modelling of membrane fouling in a submerged membrane bioreactor, J. Memb. Sci. 278 (2006) 151–161, https://doi.org/10.1016/j.memsci.2005.10.051.
[20] A. Charfi, J. Harmand, N. Ben Amar, A. Grasmick, M. Heran, Deposit membrane fouling: Influence of specific cake layer resistance and tangential shear stresses, Water Sci. Technol. 70 (2014) 40–46, https://doi.org/10.2166/wst.2014.186.
[21] A. Charfi, Y. Yang, J. Harmand, N. Ben Amar, M. Heran, A. Grasmick, Soluble microbial products and suspended solids influence in membrane fouling dynamics and interest of punctual relaxation and/or backwashing, J. Memb. Sci. 475 (2015) 156–166, https://doi.org/10.1016/j.memsci.2014.09.059.
[22] A. Charfi, N. Thongmak, B. Benyahia, M. Aslam, J. Harmand, N.Ben Amar, G. Lesage, P. Sridang, J. Kim, M. Heran, A modelling approach to study the fouling of an anaerobic membrane bioreactor for industrial wastewater treatment, Bioresour. Technol. 245 (2017) 207–215, https://doi.org/10.1016/j.biortech.2017.08.003.
[23] N. Kalboussi, J. Harmand, A. Rapaport, T. Bayen, F. Ellouze, N. Ben Amar, Optimal control of physical backwash strategy - towards the enhancement of membrane filtration process performance, J. Memb. Sci. 545 (2018) 38–48, https://doi.org/10.1016/j.memsci.2017.09.053.
[24] F. Aichouche, N. Kalboussi, A. Rapaport, J. Harmand, F. Aichouche, N. Kalboussi, A. Rapaport, J.H. Modeling, F. Aichouche, N. Kalboussi, A. Rapaport, Modeling and optimal control for production-regeneration systems - preliminary results To cite this version: HAL Id: hal-02587771 Modeling and optimal control for production-regeneration systems - preliminary results -, (2020).
[25] R.W. Field, G.K. Pearce, Critical, sustainable and threshold fluxes for membrane filtration with water industry applications, Adv. Colloid Interface Sci. 164 (2011) 38–44, https://doi.org/10.1016/j.cis.2010.12.008.
[26] N. Ghaffour, A. Qamar, Membrane fouling quantification by specific cake resistance and flux enhancement using helical cleaners, Sep. Purif. Technol. 239 (2020), https://doi.org/10.1016/j.seppur.2020.116587.
[27] J. Liang, L. Yu, J. Wu, The dynamic change of specific cake resistance in membrane bioreactor due to periodical cake relaxation, J. Environ. Chem. Eng. 8 (2020) 103837, https://doi.org/10.1016/j.jece.2020.103837.
[28] B. Benyahia, A. Charfi, G. Lesage, M. Heran, B. Cherki, J. Harmand, Coupling a Simple and Generic Membrane Fouling Model with Biological Dynamics: Application to the Modeling of an Anaerobic Membrane BioReactor (AnMBR), Membranes 14 (3) (2024) 69, https://doi.org/10.3390/membranes14030069.
[29] T. Mohammadi, A. Kohpeyma, M. Sadrzadeh, Mathematical modeling of flux decline in ultrafiltration, Desalination 184 (2005) 367–375, https://doi.org/10.1016/j.desal.2005.02.060.
[30] G. Di Bella, G. Mannina, G. Viviani, An integrated model for physical-biological wastewater organic removal in a submerged membrane bioreactor: model development and parameter estimation, J. Memb. Sci. 322 (2008) 1–12, https://doi.org/10.1016/j.memsci.2008.05.036.
[31] B. Wu, T. Kitade, T.H. Chong, T. Uemura, A.G. Fane, Role of initially formed cake layers on limiting membrane fouling in membrane bioreactors, Bioresour. Technol. 118 (2012) 589–593, https://doi.org/10.1016/j.biortech.2012.05.016.
[32] Luong, A. Mulchandani, Microbial inhibition kinetics revisited, Enzym. Microb. Technol. 11 (1989) 66–73.
[33] D. Dochain, P. Vanrolleghem, Dynamical modelling & estimation in wastewater treatment processes, 9781780403045–9781780403045, Water Intell. Online 4 (2015), https://doi.org/10.2166/9781780403045.
[34] M.D. Morris, Factorial sampling plans for preliminary computational experiments, Technometrics 33 (1991) 161–174, https://doi.org/10.1080/00401706.1991.10484804.
[35] J.C. Helton, F.J. Davis, Latin hypercube sampling and the propagation of uncertainty in analyses of complex systems, Reliab. Eng. Syst. Saf. 81 (2003) 23–69, https://doi.org/10.1016/S0951-8320(03)00058-9.
[36] A. Saltelli, S. Tarantola, F. Campolongo, M. Ratto, Sensitivity analysis in practice: a guide to assessing scientific models (Google eBook), 2004. (http://books.google.com/books?id=NsAVmohPNpQC&pgis=1f).
[37] G. Sin, K.V. Gernaey, Improving the Morris method for sensitivity analysis by scaling the elementary effects, Comput. Aided Chem. Eng. 26 (2009) 925–930, https://doi.org/10.1016/S1570-7946(09)70154-3.

[38] M.V. Ruano, J. Ribes, A. Seco, J. Ferrer, An improved sampling strategy based on trajectory design for application of the Morris method to systems with many input factors, Environ. Model. Softw. 37 (2012) 103–109, https://doi.org/10.1016/j.envsoft.2012.03.008.
[39] F. Campolongo, J. Cariboni, A. Saltelli, An effective screening design for sensitivity analysis of large models, Environ. Model. Softw. 22 (2007) 1509–1518, https://doi.org/10.1016/j.envsoft.2006.10.004.
[40] F. Campolongo, S. Tarantola, A. Saltelli, Tackling quantitatively large dimensionality problems, Comput. Phys. Commun. 117 (1999) 75–85, https://doi.org/10.1016/S0010-4655(98)00165-9.
[41] G. Sin, K.V. Gernaey, M.B. Neumann, M.C.M. van Loosdrecht, W. Gujer, Uncertainty analysis in WWTP model applications: a critical discussion using an example from design, Water Res. 43 (2009) 2894–2906, https://doi.org/10.1016/j.watres.2009.03.048.
[42] D. Banti, M. Mitrakas, G. Fytianos, A. Tsali, P. Samaras, Combined effect of colloids and SMP on membrane fouling in MBRs, Membr. (Basel) 10 (2020) 1–15, https://doi.org/10.3390/membranes10060118.
[43] A. Robles, M.V. Ruano, J. Ribes, J. Ferrer, Factors that affect the permeability of commercial hollow-fibre membranes in a submerged anaerobic MBR (HF-SAnMBR) system, Water Res. 47 (2013) 1277–1288, https://doi.org/10.1016/j.watres.2012.11.055.
[44] A. Robles, G. Capson-Tojo, M.V. Ruano, A. Seco, J. Ferrer, Real-time optimization of the key filtration parameters in an AnMBR: urban wastewater mono-digestion vs. co-digestion with domestic food waste, Waste Manag. 80 (2018) 299–309, https://doi.org/10.1016/j.wasman.2018.09.031.
[45] A. Robles, M.V. Ruano, J. Ribes, A. Seco, J. Ferrer, Model-based automatic tuning of a filtration control system for submerged anaerobic membrane bioreactors (AnMBR), J. Memb. Sci. 465 (2014) 14–26, https://doi.org/10.1016/j.memsci.2014.04.012.
[46] H. Yang, X. Yu, J. Liu, Z. Tang, T. Huang, Z. Wang, Y. Zhong, Z. Long, L. Wang, A concise review of theoretical models and numerical simulations of membrane fouling, Water (Switz.) 14 (2022), https://doi.org/10.3390/w14213537.
[47] S.S. Haramkar, G.N. Thombre, S.V. Jadhav, B.N. Thorat, The influence of particle (s) size, shape and distribution on cake filtration mechanics-a short review, C. R. Chim. 24 (2021) 255–265, https://doi.org/10.5802/CRCHIM.84.
[48] D. Bourcier, J.P. Féraud, D. Colson, K. Mandrick, D. Ode, E. Brackx, F. Puel, Influence of particle size and shape properties on cake resistance and compressibility during pressure filtration, Chem. Eng. Sci. 144 (2016) 176–187, https://doi.org/10.1016/j.ces.2016.01.023.
[49] B. Schäfer, M. Hecht, J. Harting, H. Nirschl, Agglomeration and filtration of colloidal suspensions with DVLO interactions in simulation and experiment, J. Colloid Interface Sci. 349 (2010) 186–195, https://doi.org/10.1016/j.jcis.2010.05.025.
[50] J. Liu, Y. Zhao, Y. Fan, H. Yang, Z. Wang, Y. Chen, C.Y. Tang, Dissect the role of particle size through collision-attachment simulations for colloidal fouling of RO/NF membranes, J. Memb. Sci. 638 (2021) 119679, https://doi.org/10.1016/j.memsci.2021.119679.
[51] A. Robles, M.V. Ruano, J. Ribes, A. Seco, J. Ferrer, A filtration model applied to submerged anaerobic MBRs (SAnMBRs), J. Memb. Sci. 444 (2013) 139–147, https://doi.org/10.1016/j.memsci.2013.05.021.